PHYSICAL REVIEW D VOLUME 20, NUMBER 9 1 NOVEMBER 1979

Family of relativistic deuteron wave functions

W. W. Buck
Department of Physics, State University of New York, Stony Brook, New York 11794

Franz Gross
Department of Physics, College of William and Mary, Williamsburg, Virginia 23185
(Received 22 March 1979)

We present a family of realistic relativistic deuteron wave functions obtained by numerically solving an integral equation with a π-NN coupling which is a mixture of γ^5 and $\gamma^5\gamma^\mu$ forms. We present six solutions for different values of the mixing parameter λ, varying smoothly from 0 (pure $\gamma^5\gamma^\mu$) to 1 (pure γ^5). We find that the small relativistic components of the wave function increase rapidly with λ, and we give a simple explanation for this result. In addition to π exchange, our model includes σ, ρ, and ω exchanges. Analytic forms are given for the wave functions which can be used in either position or momentum space. We discuss the validity of various nonrelativistic approximations and the convergence of the equation.

I. SUMMARY AND RESULTS

A. Introduction

In a previous letter[1] we presented two relativistic deuteron wave functions obtained by numerically solving a relativistic wave equation for the two-nucleon (NN) system. In this paper we present an entire family of such solutions, obtained with a more realistic interaction as described below.

The general structure of the wave equation has been discussed previously[2] and will be reviewed in Sec. II A below. Briefly, the equation has the property that one of the two interacting nucleons is on its mass shell (so that if p_1 is its four-momentum, $p_1^2=M^2$) while the other nucleon (with four-momentum p_2) is off-shell. In this paper we use a relativistic one-boson-exchange (OBE) model to describe the interaction between the two nucleons. OBE models have been used widely and have been found by a number of authors to give a reasonable account of the entire NN spectrum.[3] We rely on this success to provide the general justification for using such a model in this paper. However, only four bosons are included here: the π, ρ, ω and a fictitious σ chosen to simulate the bulk of the important two-pion-exchange force. The detailed form that we used for the coupling of these bosons to the nucleon is described in Sec. II C below.

Using this model, it is possible to adjust some of the OBE parameters so that the relativistic wave equation has solutions describing the deuteron. In order to reduce the arbitrariness of this procedure, all the OBE parameters except three were fixed at reasonable values. The three which were allowed to vary are the σNN coupling constant, $g_\sigma^2/4\pi$, the cutoff mass in the form factor which regulates the πNN vertex, Λ_π, and a mixing parameter, λ, in the πNN coupling.

The structure of the πNN coupling and the mixing parameter λ play a central role in our results, and will be discussed briefly now. For the πNN coupling we used

$$g_\pi\left[\lambda\gamma^5+(1-\lambda)\frac{(p_f-p_i)\cdot\gamma\gamma^5}{2M}\right], \qquad (1)$$

where g_π is the πNN coupling constant ($g_\pi^2/4\pi=14.48$) and p_f and p_i are the final and initial nucleon four-momenta. This form has the property that when $\lambda=1$ the coupling is pure γ^5, and when $\lambda=0$ the coupling is pure $\gamma^\mu\gamma^5$, and the individual terms are normalized so that if the nucleon is on-shell the coupling is completely independent of λ (the equivalence theorem[4]). However, when the nucleon is off shell the coupling does depend on λ and since one of our nucleons is off shell, each value of λ gives a different one-pion-exchange (OPE) interaction. The long-range part of this interaction corresponds to the region in momentum space where the off-shell nucleon approaches its mass shell, so that it is independent of λ, but at short range, where one of the two nucleons is far off shell, the interaction is sensitive to λ. This question will be discussed in some detail in part C of this section.

Solutions describing the deuteron were obtained for different values of λ by adjusting $g_\sigma^2/4\pi$ and Λ_π so as to obtain the correct binding energy and quadrupole moment. Solutions for values of λ between 0 and 1.0 (in steps of 0.2) are presented in part B of this section. Since these solutions are all closely related, they are viewed as a single family of wave functions.

In the final part C of this section we discuss some interesting features of this family of solutions. We make comments about the σ model as it pertains to nuclear forces, and about the validity of nonrelativistic, or semirelativistic approximations. In Sec. II we reveiw the theory briefly, and in Sec. III we discuss the numerical techniques and convergence of the numerical solutions. The full expressions for the kernels are presented in the Appendix.

Before we turn to a description of our wave functions below, we offer the following assessment. Solving for the relativistic deuteron is, of course, only a small part of the task required to fit the entire spectrum of the nucleon-nucleon system. Nevertheless, deuteron wave functions play an important role in many physical processes. Examples of such processes include elastic and inelastic e-d scattering, backward n-d scattering, and threshold $\pi + d \to p + p$. For these processes it is sometimes convenient to have a set of different relativistic wave functions, each one of which is realistic but which differ in their off-shell character. All of the wave functions presented here are realistic in the sense that they are determined from the OBE model with realistic parameters, but the nucleon-nucleon scattering phase shifts have not been calculated for any of these models. They also have different off-shell properties, as will be emphasized in part C below. Whether all of these wave functions will continue to be regarded as realistic when the entire two-nucleon spectrum is fitted with an OBE model remains to be seen.

B. The wave functions

In this part we will present our results for the wave functions as briefly as possible; for more details and precise definitions the reader is referred to Sec. II.

Each set of deuteron wave functions we obtain is composed of four wave functions:

u, the S-state wave function,

w, the D-state wave function,

v_t, the triplet-P-state wave function,

v_s, the singlet-P-state wave function.

The only wave functions which occur in nonrelativistic theories are u and w. In a relativistic framework, u and w can be thought of as the large upper components of the coupled Dirac wave functions; the smaller lower components which arise from the extra degree of freedom possessed by an off-shell Dirac particle are the P states, v_t and v_s, which are smaller by a power of v/c and which have opposite spatial parity than u and w. We wish to emphasize that the overall parity of our P states is the same as for the S and D states, just as in the more familiar case of the wave functions for a relativistic hydrogen atom, where on finds that the lower component of the ground state is also a

TABLE I. The one-boson-exchange (OBE) parameters common to the family of solutions presented in the paper. The precise form of the couplings is given in Sec. II C, with form factors normalized to unity at zero momentum transfer, as defined in Sec. II E.

Meson (B)	Mass (MeV)	$\frac{g_B^2}{4\pi}$	K_B	Λ_B (MeV)
π	138.0	14.48		varied
σ	400.0	varied		1600
ρ	770.0	0.4	6.6	1600
ω	783.0	6.0	−0.12	1600

P state. The P states were first systematically discussed by Remler,[5] and obtained in a semirelativistic calculation by Hornstein and Gross.[6]

The OBE parameters are given in Table I. Note that the OBE parameters compare reasonably with those used in other OBE models,[3] except that we have used a slightly smaller g_ρ and g_ω. Our value of g_ρ is probably uncomfortably small, and was chosen so that we could generate solutions for all values of λ. With a slightly larger g_ρ we could obtain solutions for some but not for all λ. The smaller g_ω was chosen purposely to be in better agreement with other data[7] than is usually the case with OBE models—we could easily have used a larger or smaller value without affecting the conclusions in this paper significantly. We choose $K_\rho = 6.6$ to bring our calculation into line with recent estimates of this parameter[8]; a smaller value would have allowed us to increase g_ρ.

The reduced wave functions in position space (i.e., wave function multiplied by r) are normalized according to

$$\int_0^\infty dr[u^2(r) + w^2(r) + v_t^2(r) + v_s^2(r)] = 1 , \quad (2)$$

and the normalization condition for the momentum-space wave functions (which are *not* reduced) is

$$\int_0^\infty q^2 dq[u^2(q) + w^2(q) + v_t^2(q) + v_s^2(q)] = 1 . \quad (3)$$

(Note that this normalization condition differs by a factor of $\pi/2$ from that employed in Ref. 1.) The precise definition of these wave functions and their relationship is given in Sec. II. The D-state and P-state probabilities are clearly

$$\begin{aligned} P_d &\equiv \int_0^\infty dr w^2(r) = \int_0^\infty q^2 dq w^2(q) , \\ P_t &\equiv \int_0^\infty dr v_t^2(r) = \int_0^\infty q^2 dq v_t^2(q) , \quad (4) \\ P_s &\equiv \int_0^\infty dr v_s^2(r) = \int_0^\infty q^2 dq v_s^2(q) . \end{aligned}$$

TABLE II. The OBE and deuteron parameters obtained for each member of the family of solutions discussed in the text.

λ	$\frac{g_\sigma^2}{4\pi}$	Λ_π (MeV)	$Q_{\rm NR}\left(\frac{e^2}{M_d}\right)$	$\mu_d\left(\frac{e}{2M}\right)$	P_d	P_t	P_s	ρ_D/ρ_S
0	1.928	1220	25.80	0.8530	4.74	0.03	0.00	0.0263
0.2	2.149	1400	25.80	0.8519	4.93	0.16	0.00	0.0263
0.4	3.306	1600	25.78	0.8527	4.78	0.42	0.02	0.0260
0.6	5.395	1500	25.80	0.8562	4.18	0.65	0.06	0.0258
0.8	7.744	1360	25.79	0.8584	3.79	0.91	0.13	0.0258
1.0	10.27	1235	25.80	0.8595	3.60	1.25	0.21	0.0260
Experimental			25.84±0.13	0.8574				0.0263±0.0013

The asymptotic D-to-S ratio is defined to be

$$\rho_D/\rho_S = \lim_{r\to\infty} \frac{w(r)}{u(r)}. \tag{5}$$

These quantities, together with other properties of our family of wave functions, are presented in Table II.

Note that the D-state probability is low, and fairly stable as we increase λ, but that both P-state probabilities and $g_\sigma^2/4\pi$ increase rapidly with λ. We will discuss the significance of this result in part C below. The values of the pion cutoff mass, Λ_π, are consistent with what theoretical estimates exist,[9] and also consistent with our choice of $\Lambda = 1600$ MeV for the other mesons. The parameters $g_\sigma^2/4\pi$ and Λ_π were chosen to give the correct deuteron binding energy, and experimental quadrupole moment (2.86 mb or 25.8 in our units of e/M_d^2).[10] Attention is drawn to the fact that we used the usual nonrelativistic formulas for the quadrupole and magnetic moments; relativistic formulas exist and we will report on the relativistic corrections elsewhere.

The wave functions in position space for $\lambda = 0$, 0.4, and 1 are shown in Figs. 1–3 and in momentum space in Figs. 4–6. Note that the wave functions seem to have a similar shape in all cases (except for v_s which is negative for $\lambda = 0$) and that the principal effect of increasing λ from 0 to 1 seems to be to increase v_t (and v_s) by a factor roughly proportional to λ. Attention is called to the fact that the S-state wave function in position space has a small oscillation near the origin.

In order to get a feeling for the corrections introduced by our treatment of the nuclear force, we compared our S- and D-state wave functions with those of Holinde and Machleidt. The HM2 model,[3] which uses OBE parameters similar to ours (except that it includes small η and δ contributions), gives a deuteron wave function with a 4.32% D-state probability, similar to that of the family presented here. In fact, when one compares the S- and D-state HM2 wave function with our S and D wave functions for $\lambda = 0.4$, the comparison is so close that the wave functions are practically indistinguishable (see Table III). Clearly the biggest effect of this model is the introduction of the P states rather than alteration of the shape of the S- and D-state wave functions.

In order to enable our wave functions to be easily used in other calculations, we fit our numerical solutions to a simple analytical form, which

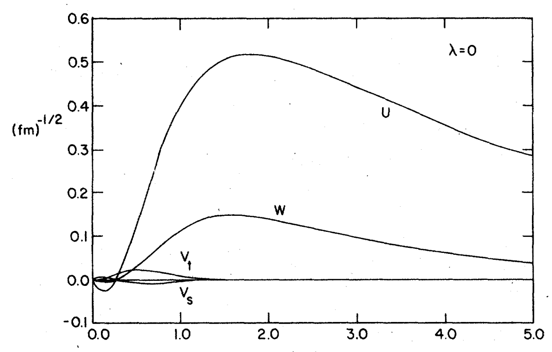

FIG. 1. The four deuteron wave functions in position space for the case $\lambda = 0$.

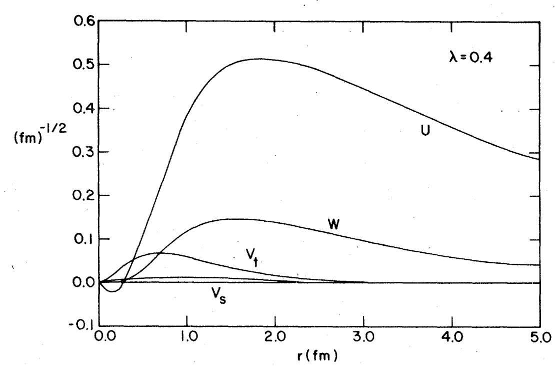

FIG. 2. The four deuteron wave functions in position space for the case $\lambda = 0.4$.

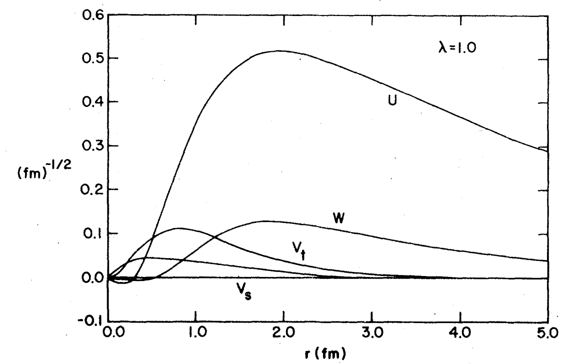

FIG. 3. The four deuteron wave functions in position space for the case λ = 1.0.

can be interpolated to give the wave function at any point. The analytical forms we use also have the property that they have the correct behavior as $r\to 0$ or $r\to\infty$ (or $q\to 0$ or ∞), and can be analytically Fourier transformed.

Let $z_l(r)$ denote any of the four reduced wave functions in position space. Then we take

$$z_l(r)=\sum_{n=0}^{N-1} b_n g_{ln}(r)\,, \tag{6}$$

where b_n are expansion coefficients determined by fitting the numerical solutions, and $g_{ln}(r)$ are a set of analytical functions with the desired properties. Our $g_{ln}(r)$ are defined as follows:

$$\begin{aligned}
g_{0n}(r)&=f_{0n}(r)-f_{0N}(r)\,,\\
g_{1n}(r)&=f_{1n}(r)-\eta_{11}f_{1N}(r)-\eta_{12}f_{1,N+1}(r)\,,\\
g_{2n}(r)&=f_{2n}(r)-\eta_{21}f_{2N}(r)-\eta_{22}f_{2,N+1}(r)\\
&\quad-\eta_{23}f_{2,N+2}(r)\,,
\end{aligned} \tag{7}$$

where the η's are implicit functions of n and will

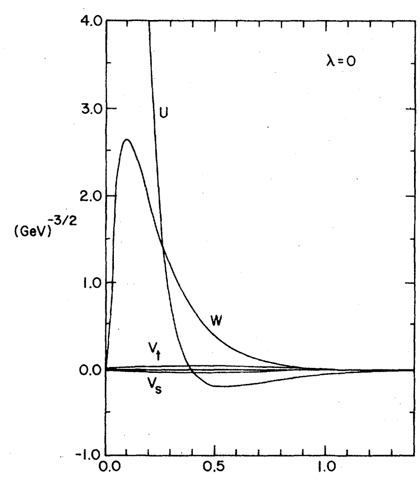

FIG. 4. The four deuteron wave functions in momentum space for the case λ = 0.

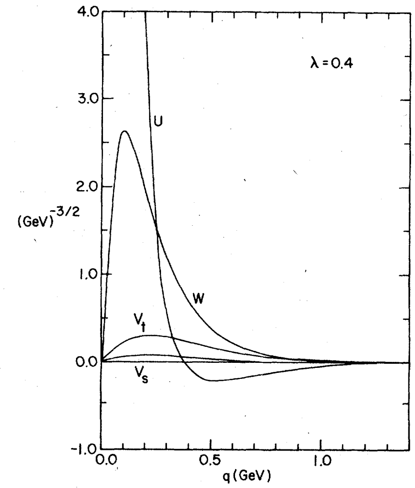

FIG. 5. The four deuteron wave functions in momentum space for the case λ = 0.4.

be discussed shortly. Introducing

$$\lambda_m=m\mu+\beta\,, \tag{8}$$

where m is an integer (equal to n, N, $N+1$, etc.) and μ and β are parameters, we have

$$\begin{aligned}
f_{0m}(r)&=e^{-\lambda_m r}\,,\\
f_{1m}(r)&=e^{-\lambda_m r}\left(1+\frac{1}{\lambda_m r}\right),\\
f_{2m}(r)&=e^{-\lambda_m r}\left(1+\frac{3}{\lambda_m r}+\frac{3}{(\lambda_m r)^2}\right).
\end{aligned} \tag{9}$$

These are the exact asymptotic forms for a wave function of angular momentum l in position space. As the reader can see, all of the wave functions are implicit functions of N (the number of terms in the expansion), β (the parameter that deter-

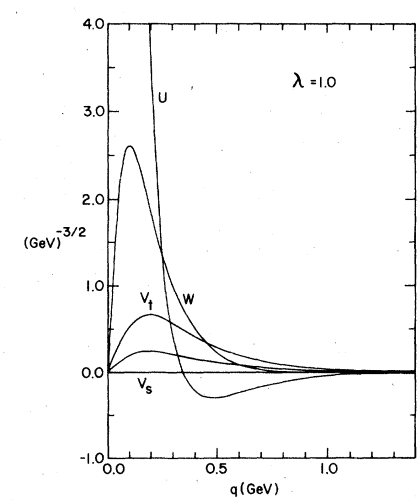

FIG. 6. The four deuteron wave functions in momentum space for the case λ = 1.0.

TABLE III. A point-by-point comparison between the S- and D-state wave functions (u and w) for our $\lambda = 0.4$ solution and the HM2 solution of Ref. 3.

r (fm)	$u_{\rm HM2}$	$u_{\lambda=0.4}$	$w_{\rm HM2}$	$w_{\lambda=0.4}$
0.2	−0.1630(−1)	−0.1805(−1)	0.2581(−2)	0.1442(−3)
0.4	0.4573(−1)	0.5237(−1)	0.1987(−1)	0.1673(−1)
0.6	0.1652	0.1710	0.4757(−1)	0.5063(−1)
0.8	0.2856	0.2889	0.7632(−1)	0.8688(−1)
1.0	0.3820	0.3828	0.1010	0.1160
1.2	0.4493	0.4480	0.1194	0.1352
1.4	0.4908	0.4882	0.1308	0.1450
1.6	0.5124	0.5090	0.1359	0.1475
1.8	0.5195	0.5161	0.1360	0.1447
2.0	0.5168	0.5137	0.1323	0.1387
2.2	0.5078	0.5051	0.1263	0.1307
2.4	0.4947	0.4925	0.1189	0.1219
2.6	0.4793	0.4774	0.1110	0.1129
3.0	0.4452	0.4436	0.9500(−1)	0.9559(−1)
4.0	0.3603	0.3586	0.6217(−1)	0.6174(−1)
5.0	0.2876	0.2861	0.4071(−1)	0.4025(−1)

mines the range of the asymptotic wave function), and μ (a parameter that determines the range of the short-range structure). The significance of β and μ suggest that a suitable choice for the u and w functions is $\beta = \sqrt{M\epsilon}$ and $\mu = m_\pi$, and this choice was taken in this paper. The P-state wave functions should have a shorter range, and this is discussed below.

The coefficients η_{li} were chosen so that each wave function would behave properly at the origin, i.e.,

$$g_{ln}(r) \underset{r\to 0}{\longrightarrow} r^{l+1} . \tag{10}$$

This requires that the η_{li} satisfy the following sum rules:

$$0 = \lambda_n^{k-l} - \sum_{i=1}^{l+1} \eta_{li} \lambda_{N+i}^{\,k-l}, \quad k = 0, 2, \ldots, 2l , \tag{11}$$

which determines the number and structure of the η's; the exact formulas are given in the end of the Appendix, Eq. (A10).

One advantage of these functions is that they can be easily transformed to momentum space. The momentum- and position-space wave functions are related by a Bessel transform:

$$\begin{aligned} z_l(q) &= \left(\frac{2}{\pi}\right)^{1/2} \int_0^\infty r dr j_l(qr) z_l(r) , \\ \frac{z_l(r)}{r} &= \left(\frac{2}{\pi}\right)^{1/2} \int_0^\infty q^2 dq j_l(qr) z_l(q) , \end{aligned} \tag{12}$$

where $j_l(qr)$ is the spherical Bessel function of order l:

$$j_l(z) = z^l \left(-\frac{1}{z}\frac{d}{dz}\right)^l \left(\frac{\sin z}{z}\right). \tag{13}$$

Hence

$$z_l(q) = \sum_{n=0}^{N-1} b_n \tilde{g}_{ln}(q) , \tag{14}$$

where $\tilde{g}_{ln}(q)$ can be obtained from Eq. (7) by introducing $\tilde{f}_{lm}(q)$ in place of $f_{lm}(r)$. We have

$$\begin{aligned} \tilde{f}_{0m}(q) &= \left(\frac{2}{\pi}\right)^{1/2} \frac{1}{q^2 + \lambda_m^{\,2}} , \\ \tilde{f}_{1m}(q) &= \left(\frac{2}{\pi}\right)^{1/2} \frac{q}{\lambda_m (q^2 + \lambda_m^{\,2})} , \\ \tilde{f}_{2m}(q) &= \left(\frac{2}{\pi}\right)^{1/2} \frac{q^2}{\lambda_m^{\,2} (q^2 + \lambda_m^{\,2})} . \end{aligned} \tag{15}$$

Each wave function is therefore completely specified in both momentum and position space by the parameters N, β, μ, and b_n. We found that $N = 8$ was sufficient in all cases, and $\mu = m_\pi$ was adequate. For β we chose $\alpha = \sqrt{M\epsilon}$ for the S- and D-state wave functions and m_π for the P-state wave functions when $\lambda \neq 0$. This is because the P-state wave functions vanish outside of the nuclear force, and hence their range should coincide with the longest range of the nuclear force. When $\lambda = 0$, however, the OPE makes a negligible contribution to the P states, and hence in this case we choose $\beta = m_\sigma = 400$ MeV. These parameters, together with the b_n's, are given in Table IV.

C. Discussion

We now turn to a discussion of some of the features of our family of solutions. We will first discuss how the dependence of the solutions on the parameter λ can be understood in terms of the structure of the theory.

TABLE IV. Tabulation of the expansion coefficients [defined in Eqs. (6) and (14)] and β parameter for v_t and v_s [Eq. (8)] for each family of wave functions. The four numbers in each box are the coefficients for u, w, v_t, and v_s in that order. In all cases the μ parameter is 138 MeV, and the β parameter for u and w is $\alpha=\sqrt{M\epsilon}$ as discussed in the text.

λ	0	0.2	0.4	0.6	0.8	1.0
β (MeV) for v_t and v_s	400	138	138	138	138	138
b_0	0.404 60	0.404 04	0.406 27	0.411 13	0.413 83	0.414 19
	$0.106\,57\times10^{-1}$	$0.106\,25\times10^{-1}$	$0.105\,89\times10^{-1}$	$0.106\,20\times10^{-1}$	$0.106\,77\times10^{-1}$	$0.107\,60\times10^{-1}$
	$-0.916\,62\times10^{-1}$	$0.397\,22\times10^{-3}$	$0.752\,80\times10^{-3}$	$0.113\,67\times10^{-2}$	$0.153\,42\times10^{-2}$	$0.193\,85\times10^{-2}$
	$-0.710\,40\times10^{-1}$	$0.169\,62\times10^{-3}$	$0.415\,66\times10^{-3}$	$0.608\,18\times10^{-3}$	$0.831\,41\times10^{-3}$	$0.108\,43\times10^{-2}$
b_1	$-0.492\,10\times10^{-1}$	$-0.487\,69\times10^{-1}$	$-0.488\,17\times10^{-1}$	$-0.498\,37\times10^{-1}$	$-0.507\,59\times10^{-1}$	$-0.515\,60\times10^{-1}$
	$-0.710\,88\times10^{-1}$	$-0.702\,49\times10^{-1}$	$-0.705\,46\times10^{-1}$	$-0.734\,40\times10^{-1}$	$-0.763\,56\times10^{-1}$	$-0.788\,28\times10^{-1}$
	$0.152\,61\times10^{1}$	$0.514\,76\times10^{-1}$	0.109 57	0.171 00	0.235 20	0.301 63
	$0.176\,62\times10^{1}$	$0.354\,56\times10^{-1}$	$0.619\,62\times10^{-1}$	$0.992\,28\times10^{-1}$	0.134 83	0.167 70
b_2	−0.161 25	−0.151 81	−0.141 80	−0.148 02	−0.161 75	−0.177 12
	−0.881 75	−0.863 68	−0.846 50	−0.830 06	−0.815 32	−0.809 67
	$-0.111\,55\times10^{2}$	−0.192 16	−0.550 89	−0.909 66	$-0.127\,81\times10^{1}$	$-0.165\,53\times10^{1}$
	$-0.205\,26\times10^{2}$	−0.436 57	−0.600 43	$-0.102\,57\times10^{1}$	$-0.137\,64\times10^{1}$	$-0.163\,62\times10^{1}$
b_3	$-0.229\,35\times10^{1}$	$-0.227\,78\times10^{1}$	$-0.241\,36\times10^{1}$	$-0.262\,26\times10^{1}$	$-0.266\,78\times10^{1}$	$-0.249\,87\times10^{1}$
	$0.392\,46\times10^{1}$	$0.380\,99\times10^{1}$	$0.354\,55\times10^{1}$	$0.293\,93\times10^{1}$	$0.234\,27\times10^{1}$	$0.192\,46\times10^{1}$
	$0.484\,07\times10^{2}$	$0.110\,24\times10^{1}$	$0.416\,30\times10^{1}$	$0.716\,35\times10^{1}$	$0.101\,75\times10^{2}$	$0.131\,58\times10^{2}$
	$0.126\,81\times10^{3}$	$0.401\,39\times10^{1}$	$0.486\,88\times10^{1}$	$0.874\,92\times10^{1}$	$0.117\,68\times10^{2}$	$0.137\,46\times10^{2}$
b_4	$0.642\,52\times10^{1}$	$0.619\,08\times10^{1}$	$0.593\,24\times10^{1}$	$0.548\,72\times10^{1}$	$0.475\,62\times10^{1}$	$0.379\,04\times10^{1}$
	$-0.160\,89\times10^{2}$	$-0.154\,57\times10^{2}$	$-0.139\,65\times10^{2}$	$-0.103\,37\times10^{2}$	$-0.658\,82\times10^{1}$	$-0.375\,28\times10^{1}$
	$-0.122\,59\times10^{3}$	$-0.207\,81\times10^{1}$	$-0.160\,92\times10^{2}$	$-0.302\,21\times10^{2}$	$-0.448\,58\times10^{2}$	$-0.594\,89\times10^{2}$
	$-0.466\,22\times10^{3}$	$-0.213\,22\times10^{2}$	$-0.237\,89\times10^{2}$	$-0.440\,41\times10^{2}$	$-0.591\,84\times10^{2}$	$-0.682\,86\times10^{2}$
b_5	$-0.150\,78\times10^{2}$	$-0.145\,85\times10^{2}$	$-0.135\,07\times10^{2}$	$-0.110\,36\times10^{2}$	$-0.800\,36\times10^{1}$	$-0.564\,40\times10^{1}$
	$0.351\,07\times10^{2}$	$0.330\,94\times10^{2}$	$0.290\,06\times10^{2}$	$0.193\,43\times10^{2}$	$0.915\,96\times10^{1}$	$0.118\,81\times10^{1}$
	$0.180\,46\times10^{3}$	$-0.198\,42\times10^{1}$	$0.346\,51\times10^{2}$	$0.714\,24\times10^{2}$	$0.110\,60\times10^{3}$	$0.150\,44\times10^{3}$
	$0.106\,83\times10^{4}$	$0.657\,97\times10^{2}$	$0.690\,93\times10^{2}$	$0.131\,06\times10^{3}$	$0.175\,91\times10^{3}$	$0.200\,61\times10^{3}$
b_6	$0.210\,48\times10^{2}$	$0.204\,16\times10^{2}$	$0.195\,13\times10^{2}$	$0.166\,44\times10^{2}$	$0.123\,23\times10^{2}$	$0.929\,77\times10^{1}$
	$-0.271\,13\times10^{2}$	$-0.248\,38\times10^{2}$	$-0.204\,46\times10^{2}$	$-0.103\,37\times10^{2}$	0.355 15	$0.889\,86\times10^{1}$
	$-0.145\,55\times10^{3}$	$0.139\,35\times10^{2}$	$-0.455\,55\times10^{2}$	$-0.104\,35\times10^{3}$	$-0.167\,93\times10^{3}$	$-0.233\,39\times10^{3}$
	$-0.153\,79\times10^{4}$	$-0.121\,38\times10^{3}$	$-0.122\,15\times10^{3}$	$-0.236\,25\times10^{3}$	$-0.316\,99\times10^{3}$	$-0.358\,36\times10^{3}$
b_7	$-0.132\,86\times10^{2}$	$-0.126\,53\times10^{2}$	$-0.123\,67\times10^{2}$	$-0.111\,29\times10^{2}$	$-0.831\,24\times10^{1}$	$-0.617\,97\times10^{1}$
	$-0.272\,64\times10^{2}$	$-0.252\,52\times10^{2}$	$-0.213\,02\times10^{2}$	$-0.121\,36\times10^{2}$	$-0.245\,52\times10^{1}$	$0.522\,90\times10^{1}$
	$0.471\,69\times10^{2}$	$-0.240\,67\times10^{2}$	$0.342\,21\times10^{2}$	$0.914\,47\times10^{2}$	$0.154\,01\times10^{3}$	$0.218\,77\times10^{3}$
	$0.135\,09\times10^{4}$	$0.131\,35\times10^{3}$	$0.128\,28\times10^{3}$	$0.251\,95\times10^{3}$	$0.338\,31\times10^{3}$	$0.380\,37\times10^{3}$

To provide a background for the discussion, it is helpful to review the structure of our wave equation. It can be written in the form[2,5]

$$-(2E-M_d)\psi^{+}=V^{++}\psi^{+}+V^{+-}\psi^{-}\,,\qquad M_d\psi^{-}=V^{-+}\psi^{+}+V^{--}\psi^{-}\,,\tag{16}$$

where E is the energy operator for a free nucleon, the potential matrix is in general a Hermitian nonlocal spin-dependent operator in momentum space, and ψ^{+} has the spin structure of a nonrelativistic deuteron wave function (containing u and w), and the spin structure of ψ^{-}, which contains v_t and v_s, will be reviewed in Sec. II B.

We will show below that the neglect of V^{--} does not introduce serious errors, and it is in any case convenient to disregard it to simplify the discussion. In this case (16) may be reduced to a more conventional form by eliminating ψ^{-}

$$-(2E-M_d)\psi^{+}=\left(V^{++}+\frac{1}{M_d}(V^{-+})^{\dagger}V^{-+}\right)\psi^{+}\,,\tag{17a}$$

$$\psi^{-}=\frac{1}{M_d}V^{-+}\psi^{+}\,.\tag{17b}$$

In Eq. (17a) we have exploited the Hermiticity of the potential matrix to write the second term in the effective potential in a form which displays its positive-definite character. This term was referred to as the quadratic potential in Ref. 2. Equation (17) will serve as a convenient starting point for our discussion.

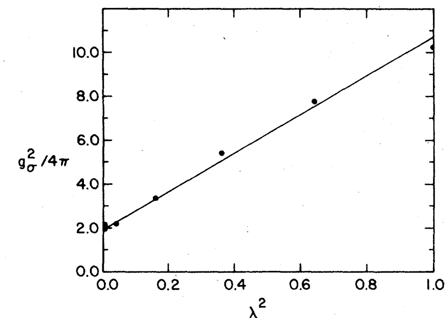

FIG. 7. The σ coupling constant vs λ^2. The dots are the six cases presented in Table II; the straight line was drawn to guide the eye.

The major differences between various members of our family of solutions, as displayed in Table II, is that both the effective σ coupling constant and P-state components increase rapidly with the mixing parameter λ. In fact, the increase in $g_\sigma^2/4\pi$ is almost linear in λ^2, as can be seen from Fig. 7. However, while the P-state probabilities grow rapidly with λ^2, their dependence on λ^2 is not quite linear, and a more precise relation is obtained for the leading expansion coefficients of v_t and v_s. The first two coefficients, which give a good account of the asymptotic form, are shown in Fig. 8, where one can see that their dependence on λ is nearly linear. [The coefficients for the $\lambda=0$ case should not be compared with the others because the mass used in the analytical form Eq. (9) is not the same.]

Both of these results can be readily understood from Eq. (17). If one calculates the V^{-+} potential in the limit where only terms of order k^2/M^2

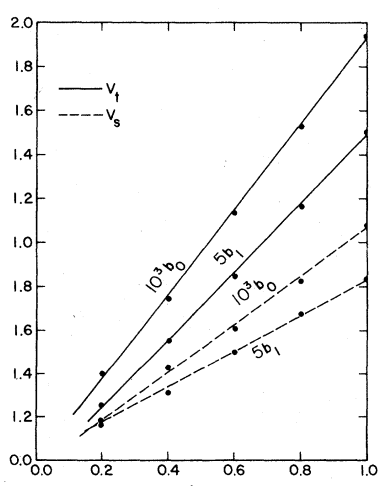

FIG. 8. The first two expansion coefficients, b_0 and b_1, for v_t and v_s vs λ. The 20 dots are the actual numbers from Table IV for the cases $\lambda \geq 0.2$. The straight lines were drawn to guide the eye.

$=(v/c)^2$ are retained (which we refer to as the semirelativistic limit), then in the OPE approximation one finds that the result is proportional to λ. This reflects the well known fact that only the off-diagonal γ^5 coupling favors transitions to negative-energy states described by ψ^-, or (in alternative language) coupling to the famous particle-antiparticle "pair" states. More precisely, it was found[6] in this limit that the long-range part of v_t and v_s are

$$\begin{aligned} v_t(r) &\cong \lambda\left(\frac{g_\pi^2}{4\pi}\right)\sqrt{3}\left(\frac{\mu}{4M^2}\right)\frac{e^{-\mu r}}{r}\left(1+\frac{1}{\mu r}\right) \\ &\quad\times[\sqrt{2}u(r)+w(r)]\,, \\ v_s(r) &\cong \lambda\left(\frac{g_\pi^2}{4\pi}\right)\sqrt{3}\left(\frac{\mu}{4M^2}\right)\frac{e^{-\mu r}}{r}\left(1+\frac{1}{\mu r}\right) \\ &\quad\times[u(r)-\sqrt{2}w(r)]\,, \end{aligned} \tag{18}$$

which is completely consistent with the results of Fig. 8. Furthermore, since the V^{-+} potential occurs squared in (17a), there is a short-range repulsion which grows with λ^2, and if this is to be counteracted by an attraction supplied by the σ, then it is also clear why the square of the σ coupling constant should grow linearly with λ^2 (Fig. 7).

An alternative explanation of linear dependence of g_σ on λ^2 comes from π-N scattering. The symmetric scattering length, defined to be the weighted average of the isospin $\frac{1}{2}$ and $\frac{3}{2}$ scattering lengths,

$$a^{(+)} \equiv -\frac{M^{(+)}}{4\pi(1+\mu/M)} = \tfrac{1}{3}(a^{(1/2)}+2a^{(3/2)})\,, \tag{19}$$

is known experimentally to be nearly zero at threshold,[11]

$$\mu a_{\rm exp}^{(+)} \cong -0.002 \pm 0.009\,. \tag{20}$$

However, the nucleon pole terms calculated with the generalized π-N coupling (1) can give quite a large value for this scattering length ($\delta \equiv \mu/2M$):

$$\begin{aligned} \mu a_{N\,\rm pole}^{(+)} &= -\frac{g_\pi^2}{4\pi}\frac{2\delta}{1+2\delta}\left(\lambda^2+\frac{\delta^2}{1-\delta^2}\right) \\ &\cong -1.88\lambda^2 - 0.010\,. \end{aligned} \tag{21}$$

The cause of this difficulty is again related to the large coupling to pair states coming from the γ^5 part of the πN coupling, and in this case one well known cure is provided by the σ. The σ meson also contributes to the symmetric scattering length

$$\mu a_\sigma^+ = \frac{g_\sigma f_\sigma}{4\pi}\frac{\mu}{m_\sigma^2}\frac{1}{1+2\delta}\,, \tag{22}$$

where f_σ is the $\sigma\pi\pi$ coupling constant, and will cancel the large result from the nucleon pole provided

$$\frac{g_\sigma f_\sigma}{m_\sigma^2} = \frac{g_\pi^2\lambda^2}{M}\,. \tag{23}$$

The well-known σ model,[12] constructed for a pure γ^5 interaction ($\lambda = 1$), has precisely this property. The σ model also gives

$$f_\sigma \cong \frac{m_\sigma^{\;2}}{M} g_\sigma , \qquad (24)$$

and inserting this result into Eq. (23) gives

$$\frac{g_\sigma^{\;2}}{4\pi} = \left(\frac{g_\pi^{\;2}}{4\pi}\right)\lambda^2 . \qquad (25)$$

Hence, a linear dependence of the σ coupling constant on λ^2 is also expected from the requirement that $a^{(+)}$ be suppressed.

Thus, from either of these points of view (which are closely related), the results of Fig. 7 are easily understood. We wish to point out, however, that no consideration of π-N scattering was built into our calculation in advance; our σ coupling constant was determined solely by the static properties of the deuteron. In this sense, our result seems to crudely suggest that a realistic deuteron cannot be obtained unless the description of π-N scattering is also realistic.

In our model, the σ meson thus provides the mechanism of pair suppression required of realistic models.[13] However, we point out that the σ does not completely suppress the pair states, or else the small wave functions v_t and v_s would be consistently small for all values of λ.

Finally, in Fig. 9 we show how the σ coupling constant depends on the pion cutoff mass if all

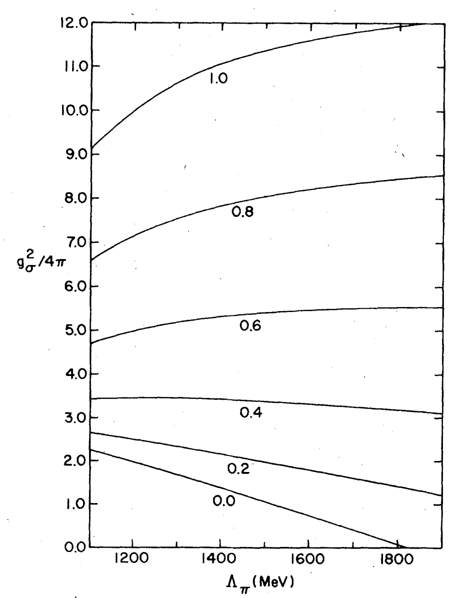

FIG. 9. Locus of points in the plane of the σ coupling constant and pion-form-factor mass for a fixed λ, which give a solution of the integral equation with the correct deuteron binding energy. The fixed value of λ corresponding to each line is labeled on the figure.

other parameters are held constant and if, for a given Λ_π, g_σ is searched until it gives a bound state at the right energy. This figure gives direct evidence for the repulsive nature of the extra quadratic term in Eq. (7a). Without this repulsive term the OPE potential is attractive, and one would therefore expect the total potential to become more attractive (primarily through the tensor force) as Λ_π increases, and therefore require a smaller g_σ. The cases for $\lambda = 0$ and 0.2 show this very clearly, but the other cases, particularly for $\lambda > 0.4$, show the opposite effect—increasing the strength of the OPE requires *more* attraction from the σ.

To verify that it is the quadratic term in (17a) which produces this repulsion, we estimate the overall effect of the central part of the potential (including the quadratic term) by calculating the volume integral of the regularized potential in the semirelativistic limit.

$$\mu^2 \int_0^\infty r^2 dr V_{eff}(\text{central}) = -\theta + \lambda^2 \frac{9}{8}\left(\frac{M}{\mu}\right)\frac{\Lambda^5(5\Lambda+1)}{(\Lambda+1)^5}\theta^2 , \qquad (26)$$

where $\theta = (g_\pi^{\;2}/4\pi)(\mu/2M)^2 = 0.08$ and $\Lambda = \Lambda_\pi/m_\pi$. Note how the second term is repulsive, and if λ is large enough the second term will dominate, making the effect of the entire potential repulsive. It is amusing that this crude estimate Eq. (26) gives a value of $\lambda_c = 0.25$ for this critical value, in fair agreement with the results of Fig. 9. A more precise estimate would require that we take account of the (attractive) tensor force, which would lead to a larger number for the critical value of λ.

Now we turn to the question of how reliable are various approximations to our relativistic equation. Two approximations we consider are

1. neglect V^{--},
2. neglect both V^{--} and V^{+-} (but not V^{-+}).

The first approximation would mean that Eq. (17) was an *exact* solution of our coupled equations, and that an equation for ψ^+ could be obtained which has precisely the same structure as a Schrödinger equation with a new effective potential including the quadratic repulsive term. The second approximation also eliminates the quadratic repulsive term and gives a Schrödinger equation for ψ^+ with only the usual V^{++} potential, and as such simulates the approach taken by almost all other investigators. We retain the potential V^{-+} in this approximation in order to estimate the size of the ψ^- wave function, which is related to meson-exchange "pair" current effects.[14]

The effect of making these two approximations is

TABLE V. Comparison of OBE and deuteron parameters when $V^{--}=0$ with exact results from Table II (labeled with an asterisk). The first row of numbers beneath the exact solution is case (a) as described in the text; the second case is (b).

λ	$\frac{g_\sigma^2}{4\pi}$	Λ_π (MeV)	$Q_{\rm NR}\left(\frac{e^2}{M_d}\right)$	$\mu_d\left(\frac{e}{2M}\right)$	P_d	P_t	P_s	ρ_D/ρ_S
0	* 1.928	1220	25.80	0.8530	4.74	0.03	0.00	0.0263
	1.942	1220	25.79	0.8531	4.72	0.04	0.00	0.0263
0.2	* 2.149	1400	25.80	0.8519	4.93	0.16	0.00	0.0263
	2.138	1450	25.80	0.8514	5.02	0.21	0.00	0.0263
	2.225	1400	25.75	0.8524	4.85	0.19	0.00	0.0262
0.4	* 3.306	1600	25.78	0.8527	4.78	0.42	0.02	0.0260
	3.489	1700	25.78	0.8529	4.76	0.52	0.02	0.0259
	3.505	1600	25.73	0.8536	4.63	0.48	0.02	0.0259
0.6	* 5.395	1500	25.80	0.8562	4.18	0.65	0.06	0.0258
	5.610	1580	25.81	0.8564	4.14	0.70	0.05	0.0257
	5.517	1500	25.65	0.8571	4.02	0.69	0.06	0.0257
0.8	* 7.744	1360	25.79	0.8584	3.79	0.91	0.13	0.0258
	7.898	1450	25.78	0.8589	3.76	0.92	0.10	0.0256
	7.609	1360	25.37	0.8597	3.56	0.94	0.13	0.0256
1.0	*10.27	1235	25.80	0.8595	3.60	1.25	0.21	0.0260
	10.39	1350	25.79	0.8598	3.56	1.20	0.17	0.0257
	9.636	1235	25.74	0.8618	3.20	1.33	0.26	0.0256

summarized in Tables V and VI. In Table V we compare the exact solution (reproduced from Table II) with the $V^{--}=0$ results for two cases: (a) when both Λ_π and g_σ are readjusted to give the correct binding energy and quadrupole moment, and (b) when Λ_π is kept the same, and only g_σ is adjusted to give the correct binding energy. In this latter case the quadrupole moment and percent D state is always lower and the percent P states are always the same or greater. Note that in either case, the effects are greater as λ increases, and the maximum error in the worst case is no more than about 5%. One sees that neglecting V^{--} introduces only a small error.

When V^{+-} is also neglected, the situation changes, and this is illustrated in Table VI. Here we present the solutions with both Λ_π and g_σ readjusted to give the correct quadrupole moment. In this case we use the nonrelativistic normalization,

$$\int_0^\infty dr(u^2+w^2)=1\ , \tag{27}$$

for all results except P_t and P_s, which are still defined as before. Our intention is to reproduce in Table VI the results of a theory which from the start neglects the ψ^- channel, and then calculates ψ^- afterwards using Eq. (17b).

Note that, although $g_\sigma^2/4\pi$ in Table VI shows a very slight dependence on λ, the dramatic dependence on λ which we saw before is absent. This is a reflection of the fact that the pair states have been suppressed from the start by simply omitting them from the equation, and hence the σ meson is no longer needed to provide the suppression. The

TABLE VI. The OBE and deuteron parameters when V^{--} and $V^{-+}=0$, as discussed in the text.

λ	$\frac{g_\sigma^2}{4\pi}$	Λ_π (MeV)	$Q_{\rm NR}\left(\frac{e^2}{M_d}\right)$	$\mu_d\left(\frac{e}{2M}\right)$	P_d	P_t	P_s	ρ_D/ρ_S
0	1.861	1190	25.81	0.8530	4.73	0.04	0.00	0.0264
0.2	1.902	1215	25.82	0.8537	4.61	0.16	0.00	0.0264
0.4	1.946	1240	25.82	0.8545	4.48	0.38	0.03	0.0265
0.6	1.979	1270	25.82	0.8551	4.36	0.71	0.09	0.0265
0.8	2.012	1300	25.81	0.8559	4.24	1.15	0.20	0.0266
1.0	2.028	1340	25.81	0.8563	4.16	1.73	0.39	0.0266

differences between Tables II and VI increase as λ increases, with the maximum effect for the case $\lambda = 1$. We see that the case in Table VI tends to give larger D and P states by as much as 50% than in Table II (or V) and, of course, much smaller values for g_σ^2. Since the P states provide an alternative way to calculate the so-called meson-exchange pair terms, which give the largest effect in most meson-exchange calculations,[14] these differences may be significant.

Our principal conclusion from this part of the discussion is that neglecting V^{--} seems not to alter things very much, while neglecting V^{+-} changes the character of the calculation, and may introduce significant differences.

We conclude this section with a few short remarks about Ref. 1. In that paper we showed that when $\lambda = 1$, there is sufficient repulsion generated by the OPE to give very reasonable deuteron wave functions—even for the simplified case when we consider *only* σ and π exchange. Unfortunately, because of a numerical error in the program, we also concluded that the same was true for the case $\lambda = 0$. However, when $\lambda = 0$ it is impossible to obtain reasonable wave functions for a deuteron with only σ and π exchange—there is simply too much attraction. For smaller λ, one needs the repulsion introduced by ρ and ω exchanges, and one must use a model similar to the ones presented here. Our result for $\lambda = 1$ in Ref. 1 was correct, and was reproduced by the present treatment, but the $\lambda = 0$ result was incorrect and should not be used.

We now turn to a more detailed account of the equation, the interactions, and the numerical techniques.

II. THEORY

A. The relativistic wave equation

For our wave equation we use the relativistic prescription of Ref. 2, where one nucleon is on its mass shell (particle 1 in this case). The wave equation is three-dimensional, and is written

$$(\tilde{\Gamma}C)_{\mu\nu}(\hat{p}) = -\int \frac{d^3k}{(2\pi)^3} V_{\mu\mu',\nu\nu'}(\hat{p},\hat{k},P) \times G_{\mu'\mu'',\nu'\nu''}(\hat{k},P)(\tilde{\Gamma}C)_{\mu''\nu''}(\hat{k}), \quad (28)$$

where μ and ν are Dirac spinor indices, $P = (M_d, 0)$ is the total energy-momentum four-vector, p and k are relative four-momenta (defined below), V is the interaction kernel with particle 1 on the mass shell, and $\tilde{\Gamma}C$ is the covariant deuteron nucleon vertex function discussed below. The two-body Green's function, G, is

$$G_{12}(k,P) = \frac{[M + \gamma\cdot(\frac{1}{2}P + \hat{k})]_1[M + \gamma\cdot(\frac{1}{2}P - \hat{k})]_2}{2E_k M_d(2E_k - M_d)}, \quad (29)$$

where the subscripts 1 and 2 denote the Dirac indices of nucleons $1(\mu'\mu'')$ and $2(\nu'\nu'')$, respectively. Since particle 1 is on shell, we impose the condition

$$(\tfrac{1}{2}P + \hat{k})^2 = (\tfrac{1}{2}P + \hat{p})^2 = M^2, \quad (30)$$

which gives $\hat{k}$ and $\hat{p}$ in terms of the three-vectors $\vec{p}$ and $\vec{k}$:

$$\hat{k} = (E_k - \tfrac{1}{2}M_d, \vec{k}), \quad \hat{p} = (E_p - \tfrac{1}{2}M_d, \vec{p}), \quad E_k = (M^2 + \vec{k}^2)^{1/2}. \quad (31)$$

The vertex function $\tilde{\Gamma}C$, where C is the Dirac charge-conjugation matrix, is related to the Blankenbecler and Cook vertex ΓC[15] by

$$(\Gamma C)_{\nu\mu} = (\tilde{\Gamma}C)_{\mu\nu}, \quad (32)$$

where we remind the reader that the Dirac index μ is associated with (the on shell) particle 1 and ν (the off shell) particle 2. It is often convenient to represent ΓC (or $\tilde{\Gamma}C$) as a matrix in Dirac space, in which case (32) implies

$$\begin{aligned}\Gamma &= C^T\tilde{\Gamma}^T C^{-1} \\ &= -C\tilde{\Gamma}^T C^{-1} \\ &\equiv F\gamma\cdot\xi + \frac{G}{M}\hat{p}\cdot\xi - \frac{M - \gamma\cdot p_2}{M}\left(H\gamma\cdot\xi + \frac{I}{M}\hat{p}\cdot\xi\right), \quad (33)\end{aligned}$$

where ξ is the four-vector polarization of the deuteron and $p_2 = \frac{1}{2}P - \hat{p}$ is the four-momentum of the off-shell particle (particle 2) which is to be multiplied from the left in Eq. (33). The four invariant functions F, G, H, and I will sometimes be referred to collectively by F_i, where $i = 1, 2, 3, 4$, respectively. They are all functions of the only scalar variable not fixed by energy-momentum conservation, p_2^2. Blankenbecler and Cook showed that (33) is the most general form of the vertex with particle 2 off shell.

The interaction kernel V will be discussed in part C below; for now we will use the fact that in an OBE model V has the form

$$V = \sum_B V_B(\hat{p},\hat{k},P)\Lambda_1^{(B)}\Lambda_2^{(B)}, \quad (34)$$

where B is summed over the four bosons π, σ, ρ, and ω, V_B is a scalar function, and Λ_1 and Λ_2 are Dirac matrices in the space of particles 1 and 2 which describe the spin interaction of the exchanged boson with the nucleons. Using this form, we may reduce Eq. (28) to a convenient matrix form:

$$\Gamma(\hat{p}) = \sum_B \int \frac{d^3k}{(2\pi)^3} \frac{V_B(\hat{p},\hat{k},P)}{2E_k M_d(2E_k - M_d)} \times \{\Lambda_2[M + \gamma\cdot(\tfrac{1}{2}P - \hat{k})]\Gamma(\hat{k})[M - \gamma\cdot(\tfrac{1}{2}P + \hat{k})]\bar{\Lambda}_1\}, \quad (35)$$

where

$$\tilde{\Lambda}_1 = C\Lambda_1^T C\,. \qquad (36)$$

Finally, substituting the form (33), multiplying out the Dirac matrices, and integrating over $d\Omega_k$, which can be done analytically, we can reduce Eq. (35) to a matrix integral equation of the general form

$$F_i(p) = \int_0^\infty dk K_{ij}(p,k) F_j(k)\,, \qquad (37)$$

where the F_i stands for F, G, H, and I as discussed above.

Equation (37) was solved numerically to obtain the results discussed in Sec. I. The numerical techniques are discussed in Sec. III, and explicit formulas for the kernels K_{ij} are given in the Appendix. In the next part below we describe how the wave functions are related to the invariants obtained directly from (37).

B. The relativistic wave functions

In this part we briefly review the definition of the relativistic wave functions and their relationship to the invariants F, G, H, and I.

The wave functions for the deuteron have been discussed in Refs. 1, 2, and 6. The common definition adopted in all these references is

$$\begin{aligned}\psi^+_{rs}(\vec{p}) &= \frac{M}{[2M_d(2\pi)^3]^{1/2}} \frac{\overline{u}^{(s)}(-\vec{p})\Gamma C \overline{u}^{(r)T}(\vec{p})}{E_p(2E_p - M_d)}\,,\\ \psi^-_{rs}(\vec{p}) &= -\frac{M}{[2M_d(2\pi)^3]^{1/2}} \frac{\overline{v}^{(-s)}(\vec{p})\Gamma C \overline{u}^{(r)T}(\vec{p})}{E_p M_d}\,,\end{aligned} \qquad (38)$$

where we have used the matrix representation for Γ and have therefore suppressed the Dirac indices.

The wave functions u, w, v_t, and v_s can be connected with the invariants F, G, H, and I through these equations. For the direct-product representation we choose the definition

$$\begin{aligned}\psi^+_{rs}(\vec{p}) &= \frac{1}{\sqrt{4\pi}}\Big[u(p)\vec{\sigma}_1\cdot\vec{\sigma}_2 \\ &\quad - \frac{w(p)}{\sqrt{8}}(3\vec{\sigma}_1\cdot\hat{p}\vec{\sigma}_2\cdot\hat{p} - \sigma_1\cdot\sigma_2)\Big]\chi_{1,M}\,,\\ \psi^-_{rs}(p) &= -\frac{\sqrt{3}}{\sqrt{4\pi}}\Big[v_s(p)\frac{1}{2}(\vec{\sigma}_1 - \vec{\sigma}_2)\cdot\hat{p} \\ &\quad + \frac{v_t(p)}{\sqrt{2}}\frac{1}{2}(\sigma_1+\sigma_2)\cdot\hat{p}\Big]\chi_{1,M}\,,\end{aligned} \qquad (39)$$

which differs by precisely a factor of $\sqrt{\pi/2}$ from the definition given in Ref. 6. In Eq. (39), $\hat{p}$ now stands for the unit three-vector in the $\vec{p}$ direction [and should not be confused with (31)] and $\chi_{1,M}$ ($M = 1, 0, -1$) is the spin-1 combination

$$\begin{aligned}\chi_{1,1} &= \alpha_{r'}\alpha_{s'}\,,\\ \chi_{1,0} &= \frac{1}{\sqrt{2}}(\alpha_{r'}\beta_{s'} + \beta_{r'}\alpha_{s'})\,,\\ \chi_{1,-1} &= \beta_{r'}\beta_{s'}\,.\end{aligned} \qquad (40)$$

We use the notation

$$\begin{aligned}&\alpha = \begin{pmatrix}1\\0\end{pmatrix}, \quad \beta = \begin{pmatrix}0\\1\end{pmatrix},\\ &\sigma_1 = \sigma_{rr'}, \quad \sigma_2 = \sigma_{ss'}\,.\end{aligned} \qquad (41)$$

We can transform this direct-product representation for the wave function into matrix form with the identity:

$$A_1 B_2 \chi_{1M} = \left(B\frac{\vec{\sigma}\cdot\vec{\xi}_M}{\sqrt{2}}A\ i\sigma_y\right)_{sr}\,, \qquad (42)$$

where ξ_M and $\tilde{A}$ are given by

$$\begin{aligned}&\xi_1 = \frac{-1}{\sqrt{2}}(1, i, 0), \quad \xi_{-1} = \frac{1}{\sqrt{2}}(1, -i, 0)\,.\\ &\xi_0 = (0, 0, 1)\,,\\ &\tilde{A} = \sigma_y A^T \sigma_y\,.\end{aligned} \qquad (43)$$

Using this we obtain alternative expressions for ψ^+ and ψ^-,

$$\begin{aligned}\psi^+_{rs}(\vec{p}) &= \frac{1}{\sqrt{4\pi}}\Big[u(p)\vec{\sigma}\cdot\xi \\ &\quad + \frac{w(p)}{\sqrt{2}}(3\hat{p}\cdot\xi\vec{\sigma}\cdot\hat{p} - \vec{\sigma}\cdot\xi)\Big]\frac{i\sigma_y}{\sqrt{2}}\Big|_{sr}\,,\\ \psi^-_{rs}(\vec{p}) &= \frac{\sqrt{3}}{\sqrt{4\pi}}\Big[v_s(p)\hat{p}\cdot\xi \\ &\quad - \frac{v_t(p)}{\sqrt{2}}(\vec{\sigma}\cdot\hat{p}\vec{\sigma}\cdot\xi - \hat{p}\cdot\xi)\Big]\frac{i\sigma_y}{\sqrt{2}}\Big|_{sr}\,.\end{aligned} \qquad (44)$$

Using this 2×2 matrix form, we obtain the desired relations directly from Eq. (38) by reducing the right-hand side to 2×2 matrix form:

$$\begin{aligned}u(p) &= \frac{p^2 G(p) + M(2E_p + M)F(p)}{3\pi M\sqrt{2M_d}E_p(2E_p - M_d)} - \frac{(2M + E_p)H(p)}{3\pi M\sqrt{2M_d}E_p}\,,\\ w(p) &= \frac{\sqrt{2}[p^2 G(p) - M(E_p - M)F(p)]}{3\pi M\sqrt{2M_d}E_p(2E_p - M_d)} - \frac{\sqrt{2}(E_p - M)H(p)}{3\pi M\sqrt{2M_d}E_p}\,,\\ \left(\frac{3}{2}\right)^{1/2} v_t(p) &= \frac{pH(p)}{\pi\sqrt{2M_d}E_p M}\,,\\ \sqrt{3}v_s(p) &= \frac{-p}{\pi\sqrt{2M_d}E_p M_d}\left[F(p) - G(p) + \frac{M_d E_p}{M^2}I\right].\end{aligned} \qquad (45)$$

These equations differ again by a factor of $\sqrt{2/\pi}$ from those in Ref. 1, but are otherwise identical.

The inverse relations are

$$F(p)=\pi\sqrt{2M_d}(2E_p-M_d)\left[u(p)-\frac{1}{\sqrt{2}}w(p)+\frac{M}{p}\left(\frac{3}{2}\right)^{1/2}v_t(p)\right],$$

$$G(p)=\pi\sqrt{2M_d}(2E_p-M_d)\left[\frac{Mu(p)}{E_p+M}+\frac{1}{\sqrt{2}}w(p)\frac{M(2E_p+M)}{p^2}+\frac{M}{p}\left(\frac{3}{2}\right)^{1/2}v_t(p)\right], \quad (46)$$

$$H(p)=\pi\sqrt{2M_d}\frac{E_pM}{p}\left(\frac{3}{2}\right)^{1/2}v_t(p),$$

$$I(p)=-\pi\sqrt{2M_d}\frac{M^2}{M_d}\left[(2E_p-M_d)\left(\frac{u(p)}{E_p+M}-\frac{1}{\sqrt{2}}w(p)\frac{E_p+2M}{p}\right)+\frac{M_d}{p}\sqrt{3}v_s(p)\right].$$

The position-space wave functions are defined to be

$$\psi^+_{rs}(\vec{r})=\frac{1}{(2\pi)^{3/2}}\int d^3p\, e^{i\vec{p}\cdot\vec{r}}\psi^+_{rs}(\vec{p}),$$
$$\psi^-_{rs}(\vec{r})=\frac{1}{(2\pi)^{3/2}}\int d^3p\, e^{i\vec{p}\cdot\vec{r}}\psi^-_{rs}(\vec{p}), \quad (47)$$

which gives the direct-product representation

$$\psi^+_{rs}(\vec{r})=\frac{1}{\sqrt{4\pi}}\left[\frac{u(r)}{r}\vec{\sigma}_1\cdot\vec{\sigma}_2+\frac{w(r)}{\sqrt{8}r}(3\vec{\sigma}_1\cdot\hat{r}\vec{\sigma}_2\cdot\hat{p}-\vec{\sigma}_1\cdot\vec{\sigma}_2)\right]\chi_{1,M},$$
$$\psi^-_{rs}(\vec{r})=-\frac{i\sqrt{3}}{\sqrt{4\pi}}\left[\frac{v_s(r)}{r}\frac{1}{2}(\vec{\sigma}_1-\vec{\sigma}_2)\cdot\hat{r}+\frac{1}{\sqrt{2}}\frac{v_t(r)}{r}\frac{1}{2}(\vec{\sigma}_1+\vec{\sigma}_2)\cdot\hat{r}\right]\chi_{1,M} \quad (48)$$

or in matrix form

$$\psi^+_{rs}(r)=\frac{1}{\sqrt{4\pi}}\left[\frac{u(r)}{r}\vec{\sigma}\cdot\xi-\frac{1}{\sqrt{2}}\frac{w(r)}{r}(3\vec{\sigma}\cdot\hat{r}\hat{r}\cdot\xi-\vec{\sigma}\cdot\xi)\right]\frac{i\sigma_y}{\sqrt{2}}\bigg|_{sr},$$
$$\psi^-_{rs}(r)=\frac{i\sqrt{3}}{\sqrt{4\pi}}\left[\frac{v_s(r)}{r}\hat{r}\cdot\xi-\frac{1}{\sqrt{2}}\frac{v_t(r)}{r}(\vec{\sigma}\cdot\hat{r}\vec{\sigma}\cdot\xi-\hat{r}\cdot\xi)\right]\frac{i\sigma_y}{\sqrt{2}}\bigg|_{sr}. \quad (49)$$

These are precisely the same definitions previously employed,[6] but the factor of $\sqrt{2/\pi}$ introduced in Eqs. (39), (44), and (45) now mean that the relations between the p-space and r-space wave functions take on a more symmetrical form than given in Ref. 6:

$$y_l(p)=\left(\frac{2}{\pi}\right)^{1/2}\int_0^\infty r^2dr\frac{y_l}{r}(r)j_l(pr),$$
$$\frac{y_l(r)}{r}=\left(\frac{2}{\pi}\right)^{1/2}\int_0^\infty p^2dp\, y_l(p)j_l(pr), \quad (50)$$

where y_l stands for any of $u(l=0)$, $w(l=2)$, or v_t or $v_s(l=1)$. [Recall Eq. (12).] The normalization conditions[2,6] were given in Eqs. (2) and (3), and the factor of $2/\pi$ which occurred in the p-space condition in Ref. 6 has been eliminated.

We now turn to a discussion of the interaction kernel.

C. The relativistic interaction kernel

The interaction kernel includes terms from the exchanges of the four bosons, π, σ, ρ, and ω. As sketched in Eq. (34), they all have the form

$$V_B=V_B(\hat{p},\hat{k},P)\Lambda_1^{(B)}\Lambda_2^{(B)}=\frac{G_B\Lambda_1^{(B)}(\Delta)\Lambda_2^{(B)}(-\Delta)}{m_B{}^2-\Delta^2}F_1^BF_2^B, \quad (51)$$

where Δ is the four-momentum transferred by particle 1 to the exchanged boson

$$\Delta=\hat{p}-\hat{k}=(E_p-E_k,\vec{p}-\vec{k}), \quad (52)$$

and m_B is the boson mass, G_B the effective coupling constant, and F_i^B, the form factor at the B-N-N vertex for particle i which will be discussed below. It remains only to specify G_B and $\Lambda^{(B)}$ for each boson:

Pion:

$$G_\pi=-3g_\pi{}^2,$$
$$\Lambda^{(\pi)}(\Delta)=\left(\lambda\gamma^5+(1-\lambda)\frac{\gamma\cdot\Delta}{2M}\gamma^5\right); \quad (53)$$

σ:

$$G_\sigma=-g_\sigma{}^2,$$
$$\Lambda^{(\sigma)}(\Delta)=1; \quad (54)$$

ρ:

$$G_\rho=-3g_\rho{}^2,$$
$$\Lambda^{(\rho)}(\Delta)=\left(\gamma^\mu+\frac{iK_\rho}{2M}\sigma^{\mu\nu}\Delta_\nu\right), \quad (55)$$

where the vector indices on the Λ's are contracted to make a scalar product;

ω:

$$G_\omega=g_\omega{}^2,$$
$$\Lambda^{(\omega)}(\Delta)=\left(\gamma^\mu+\frac{iK_\omega}{2M}\sigma^{\mu\nu}\Delta_\nu\right), \quad (56)$$

where again the vector indices on the Λ's are contracted to make a scalar product.

Since particle 1 is on its mass shell, some simplifications in Λ_1 are possible by use of the Dirac equation. For the π, ρ, and ω we have

$$\Lambda_1^{(\pi)}(\Delta)=\gamma_1^5\,,$$
$$\Lambda_1^{(V)}(\Delta)=\left(\gamma^\mu(1+K_V)-\frac{K_V}{2M}(P^\mu+\hat{p}^\mu+\hat{k}^\mu\right). \tag{57}$$

We emphasize, however, that a similar simplification is not possible for particle 2.

D. Reduction of the equation

Using the above equations, Eq. (35) can be reduced to Eq. (37). Here we wish to sketch some of the steps in the reduction.

Use must be made of (36), and it must be recalled that multiplication *from the right* by a factor of $C\bar{u}^T(p)$ is implied on both sides of Eq. (35). This means that we may always reduce $\gamma\cdot P$ by working it to the far right and using the Dirac equation to reduce it to $-(M+\frac{1}{2}\gamma\cdot\hat{p})$. Recall that $P\cdot\xi=0$.

The integration over $d\phi_k$ can be done by using the following identities:

$$\frac{1}{2\pi}\int_0^\pi d\phi_k\hat{k}^\mu=aP^\mu+b\hat{p}^\mu\,,$$
$$\frac{1}{2\pi}\int_0^\pi d\phi_k\hat{k}^\mu(k\cdot\xi)=BP^\mu(\hat{p}\cdot\xi)+C\hat{p}^\mu(\hat{p}\cdot\xi)+D\xi^\mu\,, \tag{58}$$

where

$$a=\frac{E_k}{M_d}-\frac{1}{2}-\left(\frac{E_p}{M_d}-\frac{1}{2}\right)\frac{k}{p}z\,,$$
$$b=\frac{k}{p}z\,,$$
$$B=\left(\frac{E_k}{M_d}-\frac{1}{2}\right)\frac{kz}{p}-\left(\frac{E_p}{M_d}-\frac{1}{2}\right)\frac{k^2}{p^2}P_2(z)\,, \tag{59}$$
$$C=\frac{k^2}{p^2}P_2(z);\quad D=\frac{k^2}{3}[P_2(z)-1]\,,$$

and $k=|\vec{k}|$, $p=|\vec{p}|$, $z=\hat{k}\cdot\hat{p}$, and $P_2(z)$ is a Legendre polynomial.

After the ϕ integration has been performed, the integration over z can also be done. This will be described in the Appendix.

E. The form factors

For the boson-nucleon form factor we used a pole form regularized to unity *at zero momentum transfer* (this differs from the convention of many authors who normalize their form factors to unity at the meson mass). The specific form used was

$$F_i^B=\frac{\Lambda_B{}^2}{\Lambda_B{}^2-\Delta^2+(M^2-p_i{}^2)+(M^2-k_i{}^2)}\,, \tag{60}$$

where Λ_B is the cutoff mass for boson B, p_i and k_i are the four-momenta of the external and internal nucleons, respectively, and $i=1$ or 2 depending on the nucleon with which the boson in interacting. This form was adopted to improve convergence, as we discuss below, and was suggested to us by the work of Ezawa.[16]

Note that for particle 1, which is on mass shell, F reduces to the same form as the boson propagator with an effective mass squared of $\Lambda_B{}^2$, while for the off-shell particle 2 it reduces to a similar form with a momentum-dependent effective mass squared of $\Lambda_B{}^2+2M_d(E_p+E_k-M_d)$. The boson propagator plus the form factors can be conveniently decomposed into partial fractions and the z integrations done analytically. The final formulas and the results for the z integration are tabulated in the Appendix.

F. Convergence and behavior of the wave functions at large momentum[17]

We conclude this section with an examination of the convergence of our integral equations, and a self-consistent determination of the behavior of the wave functions at large momentum.

For simplicity, first consider the spinless case with the exchange of one boson, where our integral equation would be

$$\Gamma(p)=\frac{g_B{}^2}{(2\pi)^3}\int\frac{d^3kM}{E_k(2E_k-M_d)}\frac{\Lambda_B{}^{4\epsilon}}{(m_B{}^2-\Delta^2)(\Lambda_B{}^2-\Delta^2)^\epsilon(\Lambda_{B_2}{}^2-\Delta^2)^\epsilon}\Gamma(k)\,, \tag{61}$$

where

$$\Delta^2=2M^2-2E_pE_k+2\vec{p}\cdot\vec{k}\,,$$
$$\Lambda_{B_2}{}^2=\Lambda_B{}^2+2M_d(E_p+E_k-M_d)\,, \tag{62}$$

and $\epsilon>0$ is the power falloff of the form factor. The object is to see how large ϵ must be before we are guaranteed that (61) converges.

If the integral on the right-hand side of (61) converges, then we may examine it when p is very large, obtaining the estimate

$$\Gamma(p) \cong \left(\frac{1}{2p}\right)^{1+2\epsilon} \frac{g_B^{\,2}}{4\pi^2} \int_0^\infty \frac{k^2 dk M \Gamma(k)}{E_k(2E_k - M_d)} \int_{-1}^{+1} dz \frac{\Lambda_B^{\,4\epsilon}}{(E_k - kz)^{1+\epsilon}(E_k + M_d - kz)^\epsilon} = \left(\frac{1}{2p}\right)^{1+2\epsilon} C\,. \tag{63}$$

This will then be the asymptotic behavior of Γ provided ϵ is large enough so that the constant C exists. To see if C exists, we look at the large-k behavior of its integrand. When k is large, we note that the z integration peaks very strongly at $z=1$, so that we may approximate the integral by taking $z=1$ in the slowly varying part:

$$\lim_{k\to\infty} \int_{-1}^{+1} dz \frac{\Lambda_B^{\,4\epsilon}}{(E_k - kz)^{1+\epsilon}(E_k + M_d - kz)^\epsilon} \cong \frac{\Lambda_B^{\,4\epsilon}}{M_d^\epsilon} \frac{1}{k\epsilon} \frac{1}{(E_k - k)^\epsilon} \cong \frac{\Lambda_B^{\,4\epsilon}}{M_d^\epsilon} \frac{1}{k\epsilon}\left(\frac{2k}{M^2}\right)^\epsilon . \tag{64}$$

Hence, replacing $\Gamma(k)$ by its expected asymptotic form, the full integrand goes like

$$\text{const} \times \left(\frac{1}{k}\right)^{2+\epsilon} \tag{65}$$

indicating that it converges for $\epsilon > -1$. Note that, if we had used the conventional dipole form factor, then the z integral would have gone like $k^{2\epsilon-1}$ and the full integrand would go like k^{-2} for all ϵ. In this case, it appears that convergence cannot be improved by increasing ϵ.

With spin, the argument is a bit more involved. First, if we take the limit $p\to\infty$, detailed examination of the numerators of the kernels given in the Appendix shows that F falls off more slowly than G, H, and I,

$$F \to \left(\frac{1}{p}\right)^{2\epsilon}, \qquad G,H,I \to \left(\frac{1}{p}\right)^{1+2\epsilon}, \tag{66}$$

but the combination

$$\frac{pM_d}{M^2} I + F \to \left(\frac{1}{p}\right)^{1+2\epsilon} . \tag{67}$$

Next we check the large-k dependence of the integrands of the coefficients multiplying these leading terms, using the fact that in the large-k region, the z integration peaks near 1 as discussed above, and we can replace

$$z \cong 1 + O(k^{-2\epsilon}) . \tag{68}$$

This means that the quantities (59) can be estimated as follows:

$$\begin{aligned} &a \to -\tfrac{1}{2} + O(k^{1-2\epsilon}) ,\\ &pb \to k\\ &pB \to [-\tfrac{1}{2}k + O(k^{2-2\epsilon})] ,\\ &p^2 C \to k^2 ,\\ &D \to O(k^{2-2\epsilon}) . \end{aligned} \tag{69}$$

Examination of the term $k_{21}^{(\pi)}$, for example, gives for the coefficient

$$C_{21} \cong \text{const} \times \int^\infty dk\, k^{1-3\epsilon} , \tag{70}$$

where we have used (64), the estimate (66) for F, and (69) for D. This gives the requirement

$$\epsilon > \tfrac{2}{3} , \tag{71}$$

and when the other terms are examined, we find that all other terms converge for $\epsilon = 1$.

Finally, we must check that (66) works for finite p. Now, the problem is simple because the large k behavior of the kernel can be easily read off for finite p. Using the results for large k,

$$a,b \to k , \qquad B,C,D \to k^2 , \tag{72}$$

we obtain for the kernels involving F

$$\int_0^\infty \frac{d^3kM}{E_k(2E_k - M_d)} \frac{F(k)\Lambda_B^{\,4\epsilon} O(k^2)}{(m_B^{\,2} - \Delta^2)(\Lambda_B^{\,2} - \Delta^2)^\epsilon(\Lambda_{B_2}^{\,2} - \Delta^2)^\epsilon} \to \int^\infty \frac{dk}{k^{2\epsilon}} \frac{k^2}{k^{1+2\epsilon}} , \tag{73}$$

which converges if

$$\epsilon > \tfrac{1}{2} . \tag{74}$$

For the terms involving G, H, and I, we have one extra power of k in both the numerator and the denominator, so the situation is the same. We conclude that $\epsilon = 1$ gives a convergent set of integral equations.

Finally, from Eqs. (45) and the general result (66) and (67), we obtain the estimate

$$y_i(p) \underset{p\to\infty}{\longrightarrow} \left(\frac{1}{p}\right)^{1+2\epsilon} . \tag{75}$$

If there are cooperative cancellations, convergence could be more rapid.

III. NUMERICAL METHODS

In this section we review the numerical techniques used and discuss the numerical convergence of our solutions.

We first solved Eq. (37) numerically by converting the integration from 0 to ∞ into a discrete sum over a finite number of points, the number of which we denote by N_p. Since (37) is a 4×4 coupled integral equation, this required finding the eigenvalues and eigenvectors of a $4N_p \times 4N_p$ matrix. Once F, G, H, and I were known at the N_p points, we computed u, w, v_t, and v_s at these same points using Eq. (45). Then, instead of dealing with these functions at these discrete points, we fitted the four wave functions with the momentum-space analytical forms of Eq. (14) and (15) using N terms in the expansion. This gave un-normalized expansion coefficients of the solutions, b_n. Using the analytical forms, from which analytical expressions for the norm [Eq. (3)], Q, μ_d, and the position-space wave functions are readily obtainable, we normalized the b_n's, computed Q, μ_d, and P_d, P_t, P_s, and printed out both the momentum-space and position-space wave functions at convenient points.

There are thus three problems associated with obtaining the numerical solutions:

(i) What is the optimum choice of points to convert the integral into a discrete sum?

(ii) How many points, N_p, are needed?

(iii) How many terms, N, are needed in the analytical expansion?

We relied on the work of Chao and Jackson[18] to answer the first question. They show that the optimum way to choose the points is to first map the interval from 0 to ∞ into itself using a function of the form

$$Z=\frac{1}{4\eta}\left[\sinh^{-1}\left(\frac{k}{m_\pi+\alpha}\right)\right]^2, \tag{76}$$

where $\alpha^2=M\epsilon$ and η is an adjustable parameter (which we refer to as the scale parameter). After the integrand has been mapped, we use the Gauss-Laguerre integration procedure to determine the points Z_i (and hence k_i) and the weights W_i associated with each point Z_i.

To answer the second question, we simply increased N_p until all important parameters were stable. This was done for different values of the scale parameter η until a value of η was found for which convergence was most convincing. An example of the convergence is illustrated in Table VII for the case $\lambda=0$, and the choice $N=8$ (as discussed below). Note that convergence is not excellent, but seems believable, and $N_p=32$, $\eta=0.056$ gives the best results. These parameters were also used for all other cases presented in Table II.

Finally, the choice $N=8$ was found to be quite satisfactory for all cases. The eight expansion coefficients for each wave function were determined by a least-squares fit to the 32 points using the IMSL routine. We found that, in order to have smooth and reliable wave functions, it was necessary to considerably overdetermine the functions so that the fits would not have the freedom to deviate wildly and go through every point.

Note added in proof. The experimental value of the asymptotic D-to-S ratio given in Table II is the recent measurement of H. E. Conzetl *et al.*, Phys. Rev. Lett. 43, 572 (1979).

ACKNOWLEDGMENTS

It is a pleasure to acknowledge helpful conversations with Carl Carlson (who collaborated on Sec. II F) and Etienne Delacroix. We thank Ray Southworth, and the staff of the William and Mary computer center, for their understanding and support while this work was being done on the William and Mary computer. One of us (F.G.) wishes to acknowledge support from the National Science Foundation, Grant No. PHY 77-07409, and the other one (W.B.)

TABLE VII. Convergence of selected deuteron parameters for 16, 24, and 32 Gaussian points and three different scale parameters. The differences between successive numbers are shown in the right-hand column in each box. The last parameter shown is the leading coefficient b_0 for the D-state wave function.

	N_p	η = 0.028		0.056		0.112	
Q	16	25.95	−0.19	25.92	−0.08	26.20	−0.21
	24	25.76	+0.03	25.84	−0.04	25.99	−0.09
	32	25.79		25.80		25.90	
$\frac{g_\sigma^2}{4\pi}$	16	2.092	−0.154	1.927	+0.002	1.909	+0.009
	24	1.938	−0.004	1.929	−0.001	1.918	+0.005
	32	1.934		1.928		1.923	
P_d	16	4.761	−0.050	4.782	−0.022	4.825	−0.46
	24	4.711	+0.046	4.760	−0.019	4.779	−0.19
	32	4.757		4.741		4.760	
b_0w	16	0.024 06	−0.000 11	0.024 15	−0.000 11	0.024 59	−0.000 31
	24	0.023 95	+0.000 01	0.024 04	−0.000 05	0.024 28	−0.000 14
	32	0.023 96		0.023 99		0.024 14	

wishes to acknowledge support from the Department of Energy, Contract No. EY-76-S-02-3001.

APPENDIX

Here we collect together the results for the kernel in Eq. (37), and the η's of Eq. (7) [in Eq. (A10) below].

Each term in the kernel is the sum of four contributions from π, σ, ρ, and ω exchanges. Each of these contributions is in turn a sum of three terms arising from a partial-fraction decomposition of the boson propagator and form factors. Symbols in the following are defined at the end of the formulas.

The kernels are all of the form

$$K_{ij}=\sum_B K_{ij}^{(B)}, \quad B=\pi,\sigma,\rho,\omega$$

$$K_{ij}^{(B)}=\frac{G_B}{4\pi^2}\frac{k}{p}\frac{M}{M_d}\frac{\Lambda_B{}^4}{E_k(2E_k-M_d)}\times\left[\frac{k_{ij}^{(B)}(\chi_B/2pk)}{(\chi_{B_1}-\chi_B)(\chi_{B_2}-\chi_B)}-\frac{k_{ij}^{(B)}(\chi_{B_1}/2pk)}{(\chi_{B_1}-\chi_B)(\chi_{B_2}-\chi_{B_1})}+\frac{k_{ij}^{(B)}(\chi_{B_2}/2pk)}{(\chi_{B_2}-\chi_{B_1})(\chi_{B_2}-\chi_B)}\right], \tag{A1}$$

where

$$\chi_B=m_B{}^2+2E_pE_k-2M^2,$$

$$\chi_{B_1}=\Lambda_B{}^2+2E_pE_k-2M^2,$$

$$\chi_{B_2}=\chi_{B_1}+2M_d(E_p+E_k-M_d).$$

In the following lists for $k_{ij}^{(B)}$, the superscripts (B) and the arguments are suppressed.

1. Pion

The pion kernels are given by [λ is the mixing parameter defined in Eq. (1)]

$$\begin{aligned}
k_{11}&=\frac{D}{M}+M(b-1)-\frac{E_pM_d}{2M}b+\lambda\frac{M_dE_k}{2M}+(1-\lambda)\frac{M_d}{M}\left(E_ka+\frac{E_p}{2}\right),\\
k_{12}&=(1-\lambda)\frac{M_d}{2M^3}(E_k-E_p)D,\\
k_{13}&=\frac{M_d}{M}(2E_k-M_d)\left[\lambda a+(1-\lambda)\left(-\frac{D}{2M^2}+\frac{1}{2}-\frac{E_pE_k}{2M^2}+\frac{bp^2}{2M^2}\right)\right],\\
k_{14}&=\frac{\lambda M_d}{2M^3}(2E_k-M_d)D,\\
k_{21}&=M(2b-1-C)+(1-\lambda)\frac{M_d}{M}(E_ka-E_pB),\\
k_{22}&=\frac{D}{M}+M(C-b)+\frac{M_dE_kb}{2M}-\frac{\lambda M_d}{2M}E_pC+(1-\lambda)\frac{M_d}{M}(E_pB-\tfrac{1}{2}E_kC),\\
k_{23}&=\frac{M_d}{M}(2E_k-M_d)\{\lambda[a+\tfrac{1}{2}(1-b)]+(1-\lambda)[\tfrac{1}{2}(1+C)-b]\},\\
k_{24}&=\frac{M_d}{2M}(2E_k-M_d)\left\{b-C-(1-\lambda)\left[\frac{D}{M^2}+\frac{M_dE_p}{M^2}[B+\tfrac{1}{2}(b-C)]\right]\right\},\\
k_{31}&=\tfrac{1}{2}M(b-1)+(1-\lambda)\left[\frac{D}{2M}+\frac{M_dE_k}{2M}[a+\tfrac{1}{2}(1-b)]\right],\\
k_{32}&=\frac{\lambda D}{2M},\\
k_{33}&=\frac{\lambda M_d}{2M}(2E_k-M_d)[a+\tfrac{1}{2}(1-b],\\
k_{34}&=0,\\
k_{41}&=\tfrac{1}{2}M(b-C)+\lambda MB+(1-\lambda)\tfrac{1}{2}M(b-1),\\
k_{42}&=-\lambda MB+(1-\lambda)\left[\frac{D}{2M}+\frac{1}{2}M(C-b)+\frac{M_dE_k}{2M}[B+\tfrac{1}{2}(b-C)]\right],\\
k_{43}&=(1-\lambda)\frac{M_d}{2M}(2E_k-M_d)(a+\tfrac{1}{2}-b-B+\tfrac{1}{2}C),\\
k_{44}&=\lambda\frac{M_d}{2M}(2E_k-M_d)[B+\tfrac{1}{2}(b-C)].
\end{aligned} \tag{A2}$$

2. σ

The σ kernels were expressed in terms of another, more primitive set of kernels as follows:

$$k_{i1}^{(\sigma)}=S_{i2}+S_{i3}\,,\quad k_{i2}^{(\sigma)}=S_{i4}-S_{i3}\,,$$
$$k_{i3}^{(\sigma)}=\frac{M_d}{2M^2}(2E_k-M_d)S_{i1}\,,\quad k_{i4}^{(\sigma)}=\frac{M_d}{2M^2}(2E_k-M_d)S_{i3}\,, \tag{A3}$$

where $i=1$ to 4 as before. The S kernels are

$$S_{11}=2M(1+a)\,,\quad S_{12}=-M(b+1)-\frac{M_d^2}{2M}[a+\tfrac{1}{2}(1-b)]\,,$$
$$S_{13}=-\frac{D}{M}\,,\quad S_{14}=\frac{D}{M}\,,$$
$$S_{21}=2M[a+\tfrac{1}{2}(1-b)]\,,\quad S_{22}=-M(1+b)\,,\quad S_{23}=M(C+b)\,,$$
$$S_{24}=\frac{D}{M}+\frac{M_d^2}{2M}[B+\tfrac{1}{2}(b-C)]\quad S_{31}=M[a+\tfrac{1}{2}(1-b)]\,,\quad S_{32}=-\frac{M}{2}(1+b)\,, \tag{A4}$$
$$S_{33}=0\,,\quad S_{34}=\frac{D}{2M}\,,\quad S_{41}=S_{42}=0\,,$$
$$S_{43}=-M[B+\tfrac{1}{2}(b-C)]\,,\quad S_{44}=-\frac{M}{2}(C+b)\,.$$

3. Vector

The vector kernels were expressed in terms of exactly the same equations as (A3), except with V_{ij} replacing S_{ij} on the right-hand side. The V_{ij} were in turn constructed from still more primitive vector kernels, v_{ij}, and kernels s_{ij} which have exactly the same structure as the S_{ij} given in Eq. (A4) except with m_σ and Λ_σ replaced by m_V and Λ_V. The relationship between the V_{ij} and the v's and s's is

$$V_{11}=(1-K_V^2)v_{11}-K_V(1+K_V)v_{13}+\tfrac{1}{2}K_V^2(3-R)s_{11}-K_V(1-K_V)(s_{13}-\tfrac{1}{2}xs_{31})\,,$$
$$V_{12}=(1+K_V)v_{12}+K_V(1+K_V)[zv_{11}+\tfrac{1}{2}x(v_{32}+s_{32})]+K_V[1+\tfrac{1}{2}K_V(1-R)]s_{12}+K_V(1-K_V)(zs_{11}+s_{14})+K_V^2(zxs_{31}+xs_{34})\,,$$
$$V_{13}=(1+K_V)v_{13}+K_V[1+\tfrac{1}{2}K_V(1-R)]s_{13}\,,$$
$$V_{14}=K_V(1+K_V)zv_{13}+\tfrac{1}{2}K_V^2(3-R)s_{14}+\tfrac{1}{2}K_V(1-K_V)(xs_{34}+2zs_{13})\,,$$
$$V_{21}=(1+K_V)v_{21}-K_V(1+K_V)(v_{11}+v_{23}+s_{23})+K_V[1+\tfrac{1}{2}K_V(1-R)]s_{21}-K_V(1-K_V)(s_{11}-2s_{31})+K_V^2(2s_{13}+ys_{43})\,,$$
$$V_{22}=(1+K_V)^2v_{22}-K_V(1+K_V)(v_{12}-2v_{32}+\tfrac{1}{2}yv_{42}-zv_{21}-v_{24}+s_{12}-2s_{32}-zs_{21}-s_{24})$$
$$+K_V[2+(K_V/2)(3-R)]s_{22}-K_V^2[z(2s_{11}-4s_{31})+2s_{14}-4s_{34}+ys_{44}]\,,$$
$$V_{23}=(1+K_V)^2v_{23}-K_V(1+K_V)(v_{13}+\tfrac{1}{2}yv_{43}+s_{13}+\tfrac{1}{2}ys_{43})+K_V[2+\tfrac{1}{2}K_V(3-R)]s_{23}\,,$$
$$V_{24}=(1+K_V)v_{24}-K_V(1+K_V)(\tfrac{1}{2}yv_{44}-zv_{23}-zs_{23})+K_V[1+\tfrac{1}{2}K_V(1-R)]s_{24}$$
$$-K_V(1-K_V)(s_{14}-2s_{34}+\tfrac{1}{2}ys_{44})-K_V^2z(2s_{13}+ys_{43})\,, \tag{A5}$$
$$V_{31}=K_V[1+\tfrac{1}{2}K_V(1-R)]s_{31}\,,$$
$$V_{32}=(1+K_V)^2v_{32}+K_V[2+\tfrac{1}{2}K_V(3-R)]s_{32}+K_V(1+K_V)(zs_{31}+s_{34})\,,$$
$$V_{33}=0\,,\quad V_{34}=K_V[1+\tfrac{1}{2}K_V(1-R)]s_{34}\,,$$
$$V_{41}=-K_V(1+K_V)v_{43}+K_V(1-K_V)(s_{31}-s_{43})\,,$$
$$V_{42}=(1+K_V)v_{42}+K_V(1+K_V)(v_{32}+v_{44}+s_{32})+K_V(1-K_V)s_{44}+2K_V^2(zs_{31}+s_{34})\,,$$
$$V_{43}=(1+K_V)v_{43}+K_V[1+\tfrac{1}{2}K_V(1-R)]s_{43}\,,$$
$$V_{44}=(1-K_V^2)v_{44}+K_V(1+K_V)zv_{43}+\tfrac{1}{2}K_V^2(3-R)s_{44}+K_V(1-K_V)(s_{34}+zs_{43})\,.$$

In these formulas, K_V is the tensor coupling parameter given in Table I, R is defined below, and

$$x=4-\frac{2E_pM_d}{M^2},\quad y=\frac{2E_pM_d}{M^2},\quad z=\frac{M_dE_k}{2M^2}. \tag{A6}$$

The primitive matrix v_{ij} is

$$\begin{aligned}
v_{11}&=2M,\\
v_{12}&=2Mb-\frac{M_d^2}{M}[a+\tfrac{1}{2}(1-b)]-\frac{2M_d}{M}E_pb,\\
v_{13}&=-\frac{2D}{M},\\
v_{14}&=0,\\
v_{21}&=4Mb,\\
v_{22}&=2Mb.\\
v_{23}&=2M(C-2b),\\
v_{24}&=-\frac{2M_d^2}{M}[B+\tfrac{1}{2}(b-C)]-\frac{2M_dE_p}{M}C,\\
v_{31}&=0,\\
v_{32}&=Mb,\\
v_{33}&=v_{34}=v_{41}=0,\\
v_{42}&=2Mb,\\
v_{43}&=-2M[B+\tfrac{1}{2}(b-C)],\\
v_{44}&=-Mb.
\end{aligned} \tag{A7}$$

These equations can all be compounded quite quickly on a computer.

In all of these equations, G_B was defined in part IIC, and the dependence of the $k_{ij}^{(B)}$'s on $\chi_B/2pk$, etc. is contained in the factors a, b, B, C, D [which are integrated versions of those given in Eq. (59)], and R:

$$\begin{aligned}
a&=a(y_B)=\left(\frac{2E_k-M_d}{2M_d}\right)Q_0(y_B)-\left(\frac{2E_p-M_d}{2M_d}\right)\frac{k}{p}Q_1(y_B),\\
b&=b(y_B)=\frac{k}{p}Q_1(y_B),\\
B&=B(y_B)=\left(\frac{2E_k-M_d}{2M_d}\right)\frac{k}{p}Q_1(y_B)\\
&\quad-\left(\frac{2E_p-M_d}{2M_d}\right)\frac{k^2}{p^2}Q_2(y_B),\\
C&=C(y_B)=\frac{k^2}{p^2}Q_2(y_B),\\
D&=D(y_B)=\frac{k^2}{3}[Q_2(y_B)-Q_0(y_B)],\\
R&=R(y_B)=\frac{E_kE_p-kpy_B}{M^2},
\end{aligned} \tag{A8}$$

where y_B represents any of the variables $\chi_B/2pk$, $\chi_{B_1}/2pk$, or $\chi_{B_2}/2pk$ as required in Eq. (A1), and

$$Q_l(y_B)=\tfrac{1}{2}\int_{-1}^{1}\frac{dz\,P_l(z)}{y_B-z}. \tag{A9}$$

Finally, we record the formula for the η's used in Eq. (7):

$$\begin{aligned}
\eta_{11}&=\frac{\lambda_N}{\lambda_n}\left(\frac{\lambda_{N+1}^2-\lambda_n^2}{\lambda_{N+1}^2-\lambda_N^2}\right),\\
\eta_{12}&=\frac{\lambda_{N+1}}{\lambda_n}\left(\frac{\lambda_n^2-\lambda_N^2}{\lambda_{N+1}^2-\lambda_N^2}\right),\\
\eta_{21}&=\frac{\lambda_N^2}{\lambda_n^2}\frac{D(\lambda_n,\lambda_{N+1},\lambda_{N+2})}{D(\lambda_N,\lambda_{N+1},\lambda_{N+2})},\\
\eta_{22}&=\frac{\lambda_{N+1}^2}{\lambda_n^2}\frac{D(\lambda_N,\lambda_n,\lambda_{N+2})}{D(\lambda_N,\lambda_{N+1},\lambda_{N+2})},\\
\eta_{23}&=\frac{\lambda_{N+2}^2}{\lambda_n^2}\frac{D(\lambda_N,\lambda_{N+1},\lambda_n)}{D(\lambda_N,\lambda_{N+1},\lambda_{N+2})},
\end{aligned} \tag{A10}$$

where the λ's were defined in Eq. (8) and

$$D(a,b,c)=a^4(b^2-c^2)+b^4(c^2-a^2)+c^4(a^2-b^2).$$

[1]W. Buck and F. Gross, Phys. Lett. 63B, 286 (1976).
[2]F. Gross, Phys. Rev. D 10, 223 (1974).
[3]See, for example, K. Holinde and R. Machleidt, Nucl. Phys. A256, 479 (1976).
[4]See, for example, J. Friar, Ann. Phys. (N.Y.) 104, 380 (1977).
[5]E. A. Remler, Nucl. Phys. B42, 56 (1972).
[6]J. Hornstein and F. Gross, Phys. Lett. 47B, 205 (1973).
[7]See the discussion in A. D. Jackson, D. O. Riska, and B. VerWest, Nucl. Phys. A249, 397 (1975).
[8]G. Höhler and E. Pietarinen, Nucl. Phys. B95, 210 (1975).
[9]J. Durso and A. D. Jackson, Nucl. Phys. A282, 404 (1977).
[10]R. V. Reid and M. L. Vaida, Phys. Rev. Lett. 29, 494 (1972); 34, 1064(E) (1975).
[11]S. Weinberg, Phys. Rev. Lett. 17, 616 (1966).
[12]For a review see B. W. Lee, in *Cargèse Lectures in Physics*, edited by D. Bessis (Gordon and Breach, New York, 1972), Vol. 5, pp. 1–117.
[13]G. E. Brown, in *Nucleon-Nucleon Interactions–1977*, edited by H. Fearing, D. F. Measday, and A. Strathdee, AIP Conference Proceedings No. 41 (American Institute of Physics, New York, 1978), p. 169.
[14]F. Gross, in *Few Body Dynamics*, Proceedings of the VIIth International Conference on Few Body Problems, edited by A. N. Mitra *et al.* (North-Holland,

Amsterdam, 1976), p. 523.

[15]R. Blankenbecler and L. F. Cook, Jr., Phys. Rev. 119, 1745 (1960). Our definitions of F, G, H, and I differ slightly from those used in this reference.

[16]Z. Ezawa, Nuovo Cimento 23A, 271 (1974).

[17]The work in Sec. II F was done in collaboration with Carl Carlson.

[18]Y. A. Chao and A. D. Jackson, Nucl. Phys. A215, 157 (1973).